Chapter 8
Modeling of Optical Spectral Characteristics of Nitrides-Based Quantum-Cascade Detectors

Sergii V. Gryshchenko, Mykhailo V. Klymenko, Volodymyr V. Lysak,
Igor A. Sukhoivanov

Abstract We present the theoretical analysis of resonance quantum cascade photodetector based on GaN/AlGaN compound. Calculation of reflection, transmission spectra and optical quantum efficiency was made by semianalytical method.

8.1 Introduction

High-performance photodetectors operating at near- and mid- infrared are vital components for imaging, long haul communications etc. The intersubband photonic devises like quantum cascade lasers and detectors are very attractive for this spectral range [1]. In original case (previously), the staircase slope is obtained by increasing width of the wells in a cascade. Recently, the III–V nitride alloys have been applied for these purposes. Due to their internal piezoelectric and spontaneous polarization [2], these material allow to produce required staircase energy spectrum with constant-thickness semiconductor layers. This makes semiconductor nitrides attractive for applications as an active layer for quantum cascade devices. Quantum cascade structures based on GaN/AlGaN shows ultrafast carrier dynamics thought electron-LO-phonon interactions on intersubband transitions [2, 3]. Therefore the energy levels in cascade were designed as a phonon ladder with an energy step equal to relevant phonon energies. In this work we purpose to put detective structure in optical resonator following two aims: to improve selectivity of detector

Sergii V. Gryshchenko, Mykhailo V. Klymenko
Kharkov National University of Radio Electronics, Lenin ave. 14, Kharkov 61166, Ukraine,
e-mail: s_gryshchenko@kture.kharkov.ua

Volodymyr V. Lysak
Department of Semiconductor Physics, Chonbuk National University, 664-14, Deokjin-dong, Jeonju, 651-756, Republic of Korea

Igor A. Sukhoivanov
Department of Electronics Engineering, DICIS, University of Guanajuato, Mexico

and increase total quantum efficiency. The device should operate near $1.7\,\mu m$ wavelength (0.73 eV). Considered active quantum-cascade structure is presented on Fig. 8.1. The absorption occurs in GaN layer generating electron transition between subbands $E_1 \rightarrow E_2$. Excited carrier travels to second cascade through relaxation on LO phonons $E_2 \rightarrow E_3$, $E_3 \rightarrow E_4$ and so on. In this paper, we use parabolic band approximation for conduction band structure. Embedding of the optical resonator in detector structure leads to increasing of the quantum efficiency. Reasons of that are: (1) Better interaction of the absorptive media and electromagnetic field formed by resonator. Cavity leads to enhanced electric field in active regions which will increase absorption in GaN injector layer. (2) Resonator destroys parasitic photon modes which assist energy transitions being alternative to main ones. Such a transitions in addition to main transition lead to concurrent population of subbands and resulting Pauli blocking of electron transport (shown on Fig. 8.2). In ideal case, only one subband should be populated as a result of optical transitions. Other subbands are participated in phonon-assisted relaxations. To estimate both of these effects, we have develop mathematical model of the quantum-cascade photodetector based on the semiconductor Bloch equations and classical Helmholtz equation for electromagnetic field in the resonator. Investigated structure consists from 40 cascades each of them starts from GaN absorbing well following by 5 barrier/well stack made from AlN/$Al_{0.25}Ga_{0.75}N$. Parameters for the $Al_{0.25}Ga_{0.75}N$ was obtained from linear interpolation. The active region placed between 100 nm width AlGaN electrical contacts. The resonator mirrors are proposed as 5 stacks for top and 10 stacks for bottom mirrors TiO_2/SiO_2 DBR.

8.2 Potential Profile and Band Structure

In this paper, we consider the quantum-cased detector with the structure taken from [3]. In this structure, the active layer is 6 ML GaN single-quantum well with 4 ML AlN barriers. This is the semiconductor layer where the optical absorption is occurred mainly. The active quantum wells are delimited by the superlattice consisting of five-periods of AlN/$Al_{0.25}Ga_{0.75}N$. The role of the superlattice is extracting of electrons from one excited state in one active region and transport of them to the lower energy state of another active region. The superlattice states should have cascade structure to provide efficient extraction of electrons via phonon-mediated scattering events. Such a structure can be realized applying nitride semiconductors having internal electrical polarization caused by piezoelectric effects.

All material parameters of binary semiconductors used in this work is taken from [8]. For the $Al_{0.25}Ga_{0.75}N$ semiconductor alloy, all material parameters except the band gaps have been computed using first order interpolation formulas. The band gap have been computed applying second order interpolation formula. We use expressions for piezoelectric polarizations in binary semiconductor materials from [2]. The piezoelectric polarization in ternary materials have been computed using linear interpolation formulas.

The coordinate dependence of the piezoelectric polarization allow to obtain the electric charge distribution in the structure:

$$\rho_{piezo} = -\nabla \cdot P_{piezo} \qquad (8.1)$$

If the charge distribution is known, one can compute the potential solving the Poisson equation. Usually, the periodic boundary conditions for the potential is applied. In this case, the potential drop along one period of the structure is equal zero.

In this work, we consider simplest approach to the band structure modeling based on the single-band approximation of the kp-equation [7]. In this case, the envelope functions and subband dispersion curves are solution of the Ben-Daniel-Duke equation [4]:

$$-\frac{\hbar^2}{2}\frac{\partial}{\partial z}\frac{1}{m_\perp(z)}\frac{\partial}{\partial z}\phi_{el}(z) + E_c(z)\,\phi_{el}(z) + \frac{\hbar^2 k^2}{2m_{||}(z)}\phi_{el}(z) = E\phi_{el}(z) \qquad (8.2)$$

This equation is supplemented by the periodic boundary conditions. Both Poisson and Ben-Daniel-Duke equations have been computed numerically with finite-difference method.
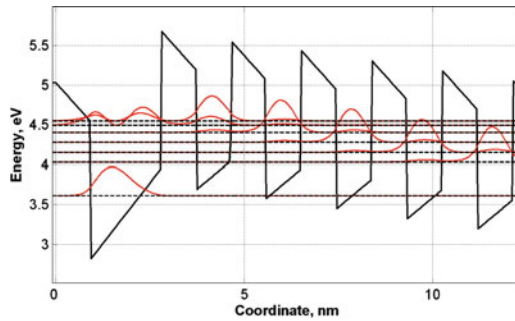
Fig. 8.1 Conduction band diagram and wave functions associated with energy levels in every well
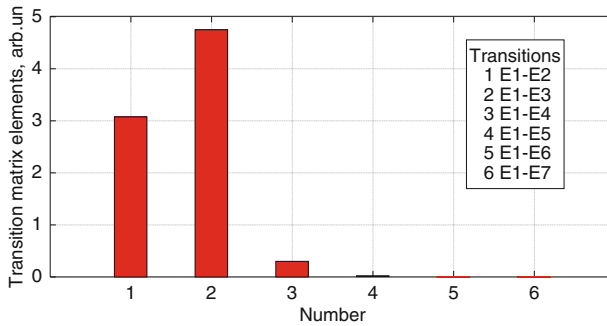
**Fig. 8.2** Dipole matrix elements for different transitions

8.3 Absorption Spectra

In this work, modeling of the absorption spectra in quantum-cascade photo-detectors is based on density matrix theory which result in the semiconductor Bloch equation [5]. Hereafter, we apply the approximation of quasi-equilibrium state in subbands. In this case, electron distribution is constant in time and approximated by the Fermi-Dirac distribution function. Therefore, this approximation allow to avoid solving of the semiconductor Bloch equations for the electron dynamics. As a result, optical properties of the photo-detector is described by the polarization equation [5]:

$$i\hbar\frac{\partial p_k}{\partial t} = (\varepsilon'_{c,k} - \varepsilon'_{v,k})p_k + (n_{c,k} - n_{v,k})\left[d_{cv}E(t) + \sum_{q\neq k} V_{|k-q|}p_q\right] + \frac{\partial p_k}{\partial t}\bigg|_{scatt} \quad (8.3)$$

$$\alpha(\omega) = \frac{1}{V}\frac{\omega}{cn}Im\left\{\frac{F\left[\sum_k d_{cv}p_k(t) + c.c.\right]}{F\left[E(t)\right]}\right\} \quad (8.4)$$

The semiconductor Bloch equations have been solved numerically applying fourth-order Runge-Kutta method. Many-body effects have been considered with Hartree-Fock approximation. This leads to renormalization of the transition energy and Rabi frequency. The scattering terms have been approximated using dephasing time computed elsewhere.
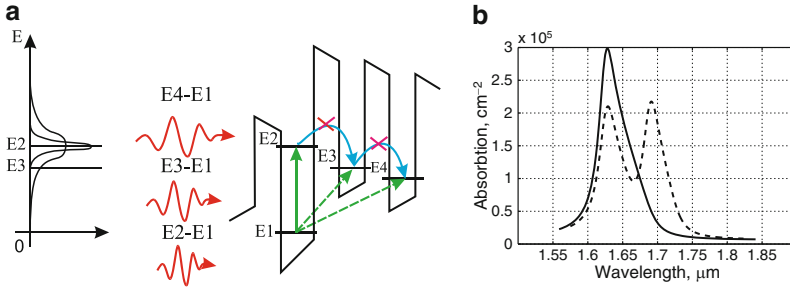
Fig. 8.3 Blocking electron transport in cascade. (a) Sketch of the optical spectra and mechanism of parasitic transitions $E_1 \rightarrow E_3$ and $E_1 \rightarrow E_4$. (b) Absorption in QCD: solid line – with cavity, dashed line – without cavity

8.4 Pauli Blocking Effect

While we have the wide spectral range of radiation directed on photodetector there are number of possible electron transitions in cascade. This lead to attenuation of the intensity of the intersubband absorption in the base quantum well in cascade. This attenuation can occur due to filling of the energy level in the next well

therefore blocking the transitions excited electrons through cascade according to Pauli principle. Analysis, based on the semiconductor Bloch equations [5], show that series of photon and phonon assisted transitions $E_1 \rightarrow E_2 \rightarrow E_3 \rightarrow E_4$ is characterized by higher probability comparing with the situation when the transition $E_1 \rightarrow E_3$ is allowed. In other words, electron transport is more intense in the case when transitions $E_1 \rightarrow E_3$ is forbidden. This effect can be treated as Pauli blocking effects [7]. Electrons collected at the subband E_2 can not transit to the subband E_3 if states of this subband are populated. Transitions $E1 \rightarrow E_3$ and $E_1 \rightarrow E_2$ lead to concurrent population of the subband E_2 and E_3.

8.5 Quantum Efficiency of the Photodetector

The formulation of quantum efficiency of resonant-cavity photodetectors always goes from the reflectivity spectral characteristic of resonator. We choose the TiO$_2$/SiO$_2$ DBR stacks for mirrors for several reasons. First, they becoming widely used in optoelectronic's as DBR mirrors due to high contrast in refractive index (3.00/1.56). This means high reflectivity by small numbers of layers and large photon-exciton coupling due to small effective cavity length. Optical reflection and absorption spectra was calculated using semianalytical transfer matrix method (TMM) [6] methodic joined with the conservation rule. We determine optical quantum efficiency (η_a) as probability of incident photon to generate an electron intersubband transition which contributes to photo-current. Therefore, one gets $\eta_a = 1 - T - R$ from energy conservation rule. The standing wave effect and multi reflections between surfaces are inherently include in TMM. In this work we have to simulate two different cases: detector with and without cavity. Optical cavity supports only one optical mode with very short bandwidth. Therefore while $E_1 \rightarrow E_3$ are partially blocked we'll obtain different absorption characteristic. Figure 8.3(b) shows absorption spectra for above mentioned cases. The cavity wavelength designed at absorption maxima on 1.628 µm.

Spectral width of the mode is less than energy gap between subbands E2 and E3. Energy of $E_2 \rightarrow E_3$ transition is near 0.03 eV. Therefore, $E_1 \rightarrow E_3 = 0.7351$ eV (1.691 µkm). Transmitting on 1.691 µkm are near 20% therefore we passively block 80% $E_1 \rightarrow E_3$ transitions. In the case when the spectrum of the radiation is wide, transitions $E_1 \rightarrow E_3$ are characterized by high probability due to high overlap integral of the wave function. Due to high reflection coefficient on non-resonance frequencies the optical quantum efficiency spectrum has only one narrow maximum (Fig. 8.4(b)). The half width of maximum equals 0.001 eV.

As a result we get 98% optical quantum efficiency on 1.628 µm central wavelength. In this paper, we have proposed to get rid of Pauli blocking effect by using high-quality cavity leading to 80% decay of the parasitic electron transitions to nearest quantum well.

In this paper, we have theoretically investigated the absorption and quantum efficiency spectral characteristics of the resonant quantum-cascade photodetector based
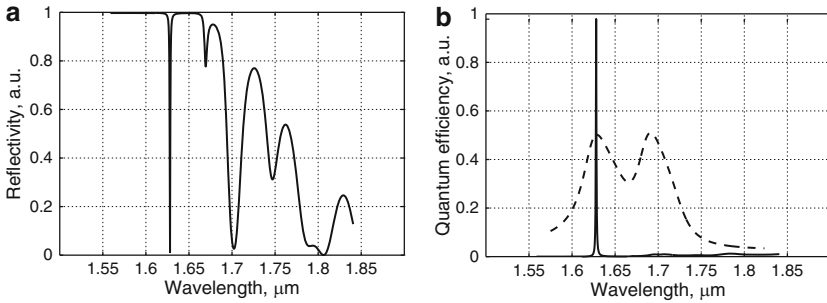
Fig. 8.4 (a) Reflectivity spectrum of the Resonant QCD. (b) Quantum efficiency in QCD with cavity (solid) and without (dashed)

on nitride compounds. The mathematical model includes piezoelectric polarization calculation, solving Ben-Daniel-Duke equation, Bloch equations and Transfer matrix method for optical part calculations. There have been shown that absorption characteristic of QCD and RQCD has differences due to concurrent population process which is treated as electronic Pauli blocking effect. The 98% quantum efficiency in RQCD was obtained due to a high-finesse TiO_2/SiO_2 DBR cavity.

References

[1] Nitride Semiconductor Devices/edited by J. Piprek, John Wiley & Sons (2007)
[2] Fiorentini, V., Bernardini, F., Ambacher, O.: Evidence for nonlinear macroscopic polarization in III-V nitride alloy heterostructures. Appl. Phys. Lett, **80**, 1204-1206 (2002)
[3] Vardia, A. et al: Near infrared quantum cascade detector in GaN/AlGaN/AlN heterostructures. Appl. Phys. Lett. **92**, 011112-1-3 (2008)
[4] Bastard, G.: Wave mechanics applied to semiconductor heterostructures. John Wiley & Sons, New York (1988)
[5] Haug, H., Koch, SW.: Quantum theory of the optical and electronic properties of semiconductors. World Scientific (2004)
[6] Gryshchenko, S. et al: Optical absorption and quantum efficiency in the resonant-cavity detector with anomalous dispersion layer. 8th International Conference on Numerical Simulation of Optoelectronic Devices. University of Nottingham, United Kingdom (1 - 5 September 2008)
[7] Chuang, S.L.: Physics of Optoelectronics devices, John Wiley & Sons (1995)
[8] Vurgafman, I. and Meyer, J.R.: Bang parameters for nitrogen-containing semiconductors. J. Appl. Phys., **94**, No. 6 (15 September 2003)